Chemosphere 260 (2020) 127582

Contents lists available at ScienceDirect

Chemosphere

journal homepage: www.elsevier.com/locate/chemosphere

Multi-pathway mercury health risk assessment, categorization and prioritization in an abandoned mercury mining area: A pilot study for implementation of the Minamata Convention

Zhidong Xu [a, b], Qinhui Lu [a, b], Xiaohang Xu [a, b], Xinbin Feng [a], Longchao Liang [c], Lin Liu [a, b], Chan Li [d], Zhuo Chen [d], Guangle Qiu [a, *]

[a] State Key Laboratory of Environmental Geochemistry, Institute of Geochemistry, Chinese Academy of Sciences, Guiyang, 550081, China
[b] University of Chinese Academy of Sciences, Beijing, 100049, China
[c] College of Resource and Environmental Engineering, Guizhou University, Guiyang, 550025, China
[d] School of Chemical and Materials Science, Guizhou Normal University, Guiyang, China

HIGHLIGHTS

- Spatial distribution of Hg concentrations in environmental media was obtained.
- A multi-pathways health risk assessment of Hg for mining areas was established.
- Risk categorization and prioritization of Hg for mining areas was conducted.
- Suggestions for the elevated exposure risks of both IHg and MeHg were provided.

GRAPHICAL ABSTRACT

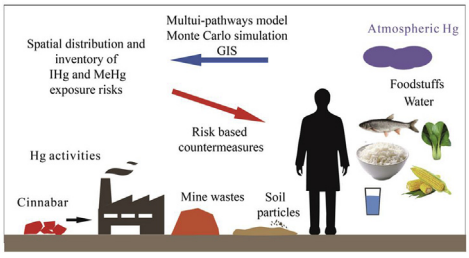

ARTICLE INFO

Article history:
Received 28 April 2020
Received in revised form
23 June 2020
Accepted 29 June 2020
Available online 10 July 2020

Handling Editor: Martine Leermakers

Keywords:
Multi-pathway exposure
Health risk assessment
Risk categorization
Hg-contaminated sites
Minamata convention

ABSTRACT

This is a systematic study of human health risk assessment (HHRA) and risk categorization for inorganic mercury (IHg) and methylmercury (MeHg) in Hg mining areas. A multi-pathway exposure model coupled with Monte Carlo simulation was constructed for the Wanshan Hg mining area (WSMM), Southwestern China, with consideration of oral ingestion (foodstuffs, water and soil), dermal contact (water and soil), and inhalation (gaseous Hg and particulate Hg). The results show that dietary intake (food and water), gaseous Hg inhalation, oral ingestion of soil particles, dermal contact, and particulate Hg inhalation comprised 88.3–96.3%, 3.49–6.14%, 0.14–5.3%, 0.02%, and <0.01% of total IHg ingestion, respectively. As expected, rice consumption contributed the highest proportion (86.3–92.7%) of MeHg. The study shows that the elevated MeHg exposure risk is the most significant issue in Hg mining areas. In addition, Hg risk categorization and prioritization in the WSMM are established for the first time based on rice-based exposure doses of IHg and MeHg. Target areas for future treatment and/or remediation are characterized according to thresholds of reference dose and provisional tolerable weekly intake for exposure doses, as well as risk screening values and risk control values for contaminated soil. The proposed multi-pathway exposure model is strongly recommended for the HHRA of Hg-contaminated sites worldwide and helps facilitate the implementation of the *Minamata Convention on Mercury*.

* Corresponding author. State Key Laboratory of Environmental Geochemistry, Institute of Geochemistry. Chinese Academy of Sciences, No. 99, Lincheng Western Road, Guanshanhu District, Guiyang, 550081, China.
E-mail address: qiuguangle@vip.skleg.cn (G. Qiu).

https://doi.org/10.1016/j.chemosphere.2020.127582
0045-6535/

1. Introduction

Mercury (Hg) is a global pollutant characterized by long-distance transportation. It comes from both natural and anthropogenic sources and can exist as elemental Hg, inorganic Hg (IHg) and organic Hg compounds in the environment. Generally, inorganic mercurial salts are absorbed at various proportions in the lungs and gastrointestinal tract, while negligible absorption occurs by dermal contact. Elemental Hg is almost completely (60–80%) absorbed by the lungs but is negligibly absorbed by both the gastrointestinal tract and skin (GnamuŠ et al., 2000; Gochfeld, 2003; USEPA, 2004). Organic Hg is absorbed by dermal contact at moderate to high degrees and is almost completely absorbed via the lungs and gastrointestinal tract (Gochfeld, 2003).

China has abundant cinnabar resources, with approximately 38% of the total national cinnabar reserve being located in Guizhou Province, Southwest China (China mineral processing technology mining website, 2017). Many Hg-contaminated sites have been generated by long-term time mining and retorting activities. In addition to Hg mining areas, gold mining areas, chemical facilities, and nonferrous metal smelting areas also are typical Hg-contaminated sites (Wang et al., 2012; Kocman et al., 2013; Eckley et al., 2020). In recent decades, many Hg health risk assessments (HHRAs) or Hg exposure risk assessment studies have been conducted in Hg mining areas (Feng et al., 2008; Zhang et al., 2010; Li, 2013; Li et al., 2015a; Du et al., 2016; Bavec et al., 2018; Jia et al., 2018; Jiménez-Oyola et al., 2020), gold mining areas (Riaz et al., 2017; Gyamfi et al., 2020), the vicinity of chemical facilities (Gibičar et al., 2009; Li et al., 2017), non-ferrous metal smelting areas (Árvay et al., 2017; Li et al., 2018), Hg-added product plants (Shao et al., 2012), and municipal solid waste incinerators (Deng et al., 2016).

In these studies, pathways of inhalation and oral ingestion, particularly rice and fish consumption, have been widely discussed. However, soil exposure pathways (oral ingestion and dermal contact) are rarely considered. In fact, individuals can orally ingest soil (or dust) particles unintentionally by outdoor hand-to-mouth activities. The oral ingestion of high-Hg-concentration soil or dust particles can pose significant exposure risks to people, especially children and toddlers (Guney et al., 2013; Safruk et al., 2015; Sun et al., 2020; Jiménez-Oyola et al., 2020). In addition, total Hg (THg) without consideration of absorption factors have usually been used directly in previous HHRA studies, which will overestimate Hg exposure risks. However, little is known about the exposure risk levels and contribution rates (CRs) of soil exposure pathways coupled with those of food and water consumption and inhalation in heavily Hg-contaminated mining areas.

Monte Carlo simulation is a random sampling method that can provide probability distributions of exposure risks. It has been extensively used in HHRA studies of heavy metal pollution of water (Dong et al., 2020), soil (Chen et al., 2019), and rice (Xu et al., 2020) in recent years. Therefore, using an optimized multi-pathway exposure model coupled with Monte Carlo simulation should provide a relatively correct and better understanding of the exposure characteristics of these pathways.

Since the *Minamata Convention on Mercury* came into force in 2017 (UNEP, 2017), HHRA studies, risk categorization, and prioritization have become essential at Hg-contaminated sites, and a pilot study of multi-pathway HHRA, risk categorization and prioritization is crucial for the implementation of the Minamata Convention. In the present study, we selected the largest Hg mining area of China as a study area and conducted a pilot study of quantitative HHRA and risk categorization. The objectives were to 1) provide a quantitative assessment of health risk levels via a multi-pathway exposure model, 2) elucidate the IHg and MeHg exposure characteristics in an Hg mining area, 3) establish Hg risk categories and priorities, and 4) link the pilot study to the implementation of the Minamata Convention.

2. Materials and methods

2.1. Study areas

The Wanshan Hg mining area (WSMM; 27° 24′–38′ N, 109° 07′–23′ E) lies in eastern Guizhou Province, Southwest China. Most large Hg mines are in the mid-western region of the WSMM. The population of the WSMM is 84,500, who mainly reside in the towns or villages of Aozhai (AZ), Gaolouping (GLP), Xiaxi (XX), Huangdao (HD), and Wanshan Town (WST), and the recent birth rate was 10.65‰, the total administrative region of WSMM is 338.13 km^2 (Wanshan Government, 2019). The large-scale Hg mining and retorting activities were stopped in 2004; however, there is an operating Hg chemical park that recycles Hg catalysts and Hg-contaminating waste.

2.2. Sampling and measurement

2.2.1. Sampling and preparation

We collected rice grain (n = 148) and surface soil (n = 86) samples and measured gaseous Hg concentrations (GEM) in ambient air (n = 67) from across the WSMM from September 2014 to October 2016. Rice grain samples were directly collected from rice paddies, thoroughly cleaned with deionized water and Milli-Q water (18.25 MΩ cm^{-1}), then freeze-dried, the hulk and bran removed, and the grain ground through a 200 mesh sieve with a pulverizer (IKA A11 Basic, Germany) before analysis. Surface dryland soil samples were collected and homogenized by mixing of three subsamples, packed in PVC bags, and then air-dried in a ventilated place and ground with a ceramic mortar through 200 mesh sieves before analysis. GEM concentrations in the atmosphere were measured by a Lumex RA-915 M^+ Zeeman modulation mercury analyzer (Lumex Company, Russia) after at least 30 min of continuous monitoring at each site, and the instrument detection limit (IDL) is 0.5 ng m^{-3}. The sampling sites are shown in Fig. S1 (a)–(c). Meanwhile, data on the THg and MeHg concentrations in drinking water (Zhang et al., 2010), vegetables (Feng et al., 2008; Zhang et al., 2010), corn (Zhang et al., 2010), pork (Feng et al., 2008), poultry (Ji et al., 2006; Zhang et al., 2010), and fish (Qiu et al., 2009) were collected. At all sampling sites, the geographic coordinates were recorded with a portable global positioning system device.

2.2.2. Hg analysis

THg. For soil, approximately 0.2 g of sample was weighed into a glass tube and digested at 95 °C with a fresh mixture of HNO_3 and HCl (1:3, v/v) for 0.5 h, then oxidized by BrCl, neutralized by NH_4OH HCl, reduced by $SnCl_2$, and measured by an F-732VJ cold vapor atomic absorption spectrometer (CVAAS; Shanghai Huaguang Instrument, China). For rice, approximately 0.2 g of sample was digested with HNO_3 at 95 °C in a water bath for 3 h, oxidized by BrCl, neutralized by NH_4OH HCl, reduced by $SnCl_2$, and measured by cold vapor atomic fluorescence spectrometer (CVAFS; Model III, Brooks Rand Co. Ltd., USA) following USEPA method 1631e (USEPA, 2002). The method blanks, sample blanks, duplicates (10%), certificated reference materials of estuary sediment (ERM CC580), and citrus leaves (GBW10020) were used to ensure data quality. Recovery of THg was in the range of 91–103% and the relative standard deviation (RSD) was <10%. The limit of detection (LOD) and quantification (LOQ) for THg analysis of CVAAS and CVAFS were 20.6 ng g^{-1} and 52.7 ng g^{-1}, 0.023 ng g^{-1} and 0.041 ng g^{-1}, respectively.

MeHg. For rice, approximately 0.2 g of rice sample was digested with 25% KOH-methanol in an oven at 75 °C for 3 h, then extracted with CH_2Cl_2 and back-extracted into the water phase, followed by $NaBEt_4$ ethylation and purging, trapping, and measured by gas chromatography-cold vapor atomic fluorescence spectrometry (GC-CVAFS; Model III, Brooks Rand Co. Ltd., USA) following method 1630 (USEPA, 2001) and Liang et al. (1996). The method blanks, sample blanks, duplicate samples (10%), and lobster hepatopancreas (Tort-2) were also used to ensure data quality. The recovery was 90–95% and the RSD was <10%. The IDL was 0.002 ng L^{-1}, method LOD and LOQ for MeHg analysis were 0.005 ng g^{-1} and 0.008 ng g^{-1}. In this study, THg and MeHg data were measured individually, while the IHg in rice and other foodstuffs was calculated as IHg = THg − MeHg.

2.3. Health risk assessment

In the conceptual multi-pathway exposure model, the pathways were characterized as 1) oral ingestion of soil particles, drinking water, and food (fish, meat, rice, other crops, and vegetables), 2) inhalation of GEM and particulate Hg (PHg), and 3) dermal contact with water and soil particles. Since the proportions of MeHg as THg (MeHg%) in drinking water (Zhang et al., 2010) and agricultural soil (Qiu et al., 2005) are approximately < 0.1%, the MeHg exposure doses via oral ingestion and dermal contact with water and soil were considered negligible. We assumed that taking a shower would be the major source of dermal contact with water, and only considered IHg because of the very low MeHg% (0.12%) in water. In this study, the PHg emitted from surface soil was used to estimate the PHg in the atmosphere by the method recommended by MEE (2014). Meanwhile, due to a lack of daily intake rate (IR) data for food consumption by children, paired exposure doses were not considered either.

In this model, we assumed that all foodstuffs supplied to residents came from local areas and that residents did not move during their lifetime. The provisional daily intake (PDI) and absorption factors were used to represent exposure risk levels following USEPA (2019a), Khpalwak et al. (2019), and Sun et al. (2020). In addition, for the PHg inhalation and dermal contact pathways, the calculations of IR were modified from the methods recommended by the USEPA (2019a). Values of exposure factors of the Chinese population were used where possible, and the RfD (MeHg 0.1 mg kg^{-1} d^{-1}, IHg 0.3 mg kg^{-1} d^{-1}) and provisional tolerable weekly intake (PTWI, converted to daily intake, MeHg 0.23 mg kg^{-1} d^{-1}, IHg 0.57 mg kg^{-1} d^{-1}) recommended by the USEPA (2019b) and JECFA (2010) were also used as criteria. The general equations were as follows:

$$PDI_i = C_i \times IR_i \times ED \times EF \times RBa_i \times CF / (BW \times AT) \quad (1)$$

$$IR_{inh-p} = IR_{inh} \Big/ PEF \quad (2)$$

$$IR_{der-s} = Adh_{event} \times SER \times SA \times EV \quad (3)$$

$$IR_{der-w} = K_p \times t_{event} \times SA \times EV \quad (4)$$

In these equations, PDI_i is the daily exposure dose via the three pathways; C_i is the concentration of pollutant in environmental media; IR_i is the daily intake rate; EF is exposure frequency; ED is exposure duration; Rba_i is relative bioaccessibility; BW is body weight; AT is exposure time ($ED \times 365$); PEF is the particle emission factor; SA is body surface area; SER is the ratio of exposure area as SA; EV is exposure frequency; Adh_{event} is the adherence rate of soil to skin; Kp is the dermal permeability coefficient, and t_{event} is the event duration. Detailed information on these parameters is listed in Table S1.

2.4. Data process and analysis

In this study, the distributions of Hg concentrations in soil, rice and soil were predicted automatically by Anderson-Darling, Kolmogorov-Smirnov, and Chi-squared test in Crystal Ball 11.2.4 (Oracle Co. Ltd., USA) embedded in Microsoft Excel (2013) (Microsoft Co. Ltd., USA). Origin 2020 (learn edition) was used to calculate the values of geometric mean (GM), arithmetic mean (AM), and median, and plot the frequency histograms. Adobe Illustrator CS6 (Adobe Co. Ltd., USA) and ArcGIS 10.2 (ESRI, USA) software were used to generate maps of the sampling sites and the spatial distribution of Hg concentrations and exposure doses. Crystal Ball 11.2.4 was used as the Monte Carlo simulation tool to calculate the PDIs and CRs.

3. Results and discussion

3.1. Hg concentrations and spatial distribution

3.1.1. Hg concentrations

Rice. The THg and MeHg concentrations in rice are listed in Table 1. THg ranged from 2.65 to 455 ng g^{-1} (lognormal) with a mean of 16.5 ± 2.31 ng g^{-1} (geometric mean ± standard deviation, GM ± SD). The highest THg value in rice was obtained from the vicinity of a chemical facility and may be due to previous mining or active Hg chemical production. Approximately 32.4% of rice samples exceeded the maximum Hg concentration allowable for cereal products (20 ng g^{-1}; NHC, 2017). The MeHg concentrations in rice ranged from 0.45 to 87.9 ng g^{-1} (lognormal) with an mean of 4.94 ± 2.60 ng g^{-1} (GM ± SD). However, the highest MeHg concentration in rice was found near a Hg mine but far away from the WST, which is quite different from the distribution of rice THg.

Drinking water and other foodstuffs. In this study, the collected Hg concentrations in drinking water, vegetables, and meat (pork, poultry, and fish) are listed in Table 1. Among these foodstuffs, the average THg concentrations in fish, pork, poultry, and vegetables were much higher, while the average THg in corn was the lowest (2.3 ng g^{-1}). Both THg and MeHg in local farmed fish were the highest (290 ng g^{-1} and 60 ng g^{-1}), while the average MeHg in drinking water and vegetables were the lowest (0.064 ng L^{-1} and 0.097 ng g^{-1}).

Soil. Soil THg concentrations ranged from 0.05 to 335 mg kg^{-1} (lognormal) with an mean of 2.7 ± 8.7 mg kg^{-1} (GM ± SD; Table 1). The highest value was observed in a vegetable cropping area near active chemical facilities in the Wanshan Hg recycling industrial park, while lower values were observed in far-away areas, including sites in XX, HD, and GLP villages. For the whole area, the THg concentrations of approximately 27.9% and 25.6% of soil samples exceeded the recent risk screening value of 3.4 mg kg^{-1} and the risk control value of 6.0 mg kg^{-1} for agricultural soil (MEE, 2018a), respectively.

Air. The GEM concentrations ranged from 1.3 to 799 ng m^{-3} (lognormal) with mean of 16.4 ± 3.0 ng m^{-3} (GM). The highest GEM concentration was measured near an active chemical facility, while much lower values were observed at sites in XX, GLP, HD, and AZ villages, which are far away from Hg mines and chemical plants. Among these sampling sites, the GEM at three sites (4.2%) exceeded the reference concentration of 300 ng m^{-3} set by the USEPA (2019b) and 9.86% of sampling sites exceeded the *China Ambient Air Quality Standard* of 50 ng m^{-3} (MEE, 2012).

Table 1
Hg concentrations in contaminated environment media from Wanshan.

Media	Hg	N	Range	AM[a]	GM[b]	Median	Sources
Soil (mg kg^{-1})	THg	86	0.05–335	21.2 ± 56.4	2.25 ± 8.63	1.35	This study
Atmosphere (ng m^{-3})	GEM	67	1.26–799	42.8 ± 118	16.4 ± 2.95	15.1	This study
Rice (ng g^{-1}, dw)	THg/MeHg	148	2.65–455/**(0.45–87.9)**[c]	25.7 ± 42.8/**(8.21 ± 11.5)**	16.5 ± 2.31/**(4.94 ± 2.60)**	15.9/**(4.86)**	This study
Water (ng L^{-1})	THg/MeHg	–	–	50/**(0.064)**	–	–	Zhang et al. (2010)
Corn (ng g^{-1}, dw)	THg/MeHg	–	–	2.3/**(0.25)**	–	–	Zhang et al. (2010)
Vegetables (ng g^{-1}, ww)	THg	–	–	130/**(0.097)**	–	–	Feng et al. (2008); Zhang et al. (2010)
Pork (ng g^{-1}, ww)	THg/MeHg	7	7.5–565/**(0.05–3.43)**	216 ± 230/**(0.85 ± 1.23)**	–	–	Feng et al. (2008)
Fish (ng g^{-1}, ww)	THg/MeHg	12	61-680/**(24–98)**	290 ± 16/**(60 ± 26)**	–	–	Qiu et al. (2009)
Poultry (ng g^{-1}, ww)	THg/MeHg	–	–	160/**(2.4)**	–	–	Ji et al. (2006), Zhang et al. (2010)

[a] AM is arithmetic mean.
[b] GM is geometric mean.
[c] Data in bold is MeHg.

3.1.2. Spatial distribution

The inverse distance weighted method was used to obtain the spatial distribution of Hg in soils, air, and rice (Fig. 1). In soil, GEM, and rice, elevated Hg concentrations were concentrated in WST and areas adjacent to Hg mines and active chemical facilities, while lower Hg concentrations were observed in areas distant from Hg mine and retorting sites. Meanwhile, the Hg concentrations in soil, air, and rice showed large variations, of 2–4 orders of magnitude, which may mean there are large variations in health risk. Hence, using WST as the base point, two circular zones with high and low Hg concentrations (with radii of about 0–4 km and 4–15 km, respectively; Fig. S1) were defined in the following risk assessment.

3.2. Hg exposure doses

3.2.1. Oral ingestion

Foodstuffs and drinking water. The PDIs for consumption of all types of foodstuffs are listed in Table 2. For IHg, the PDIs of rice

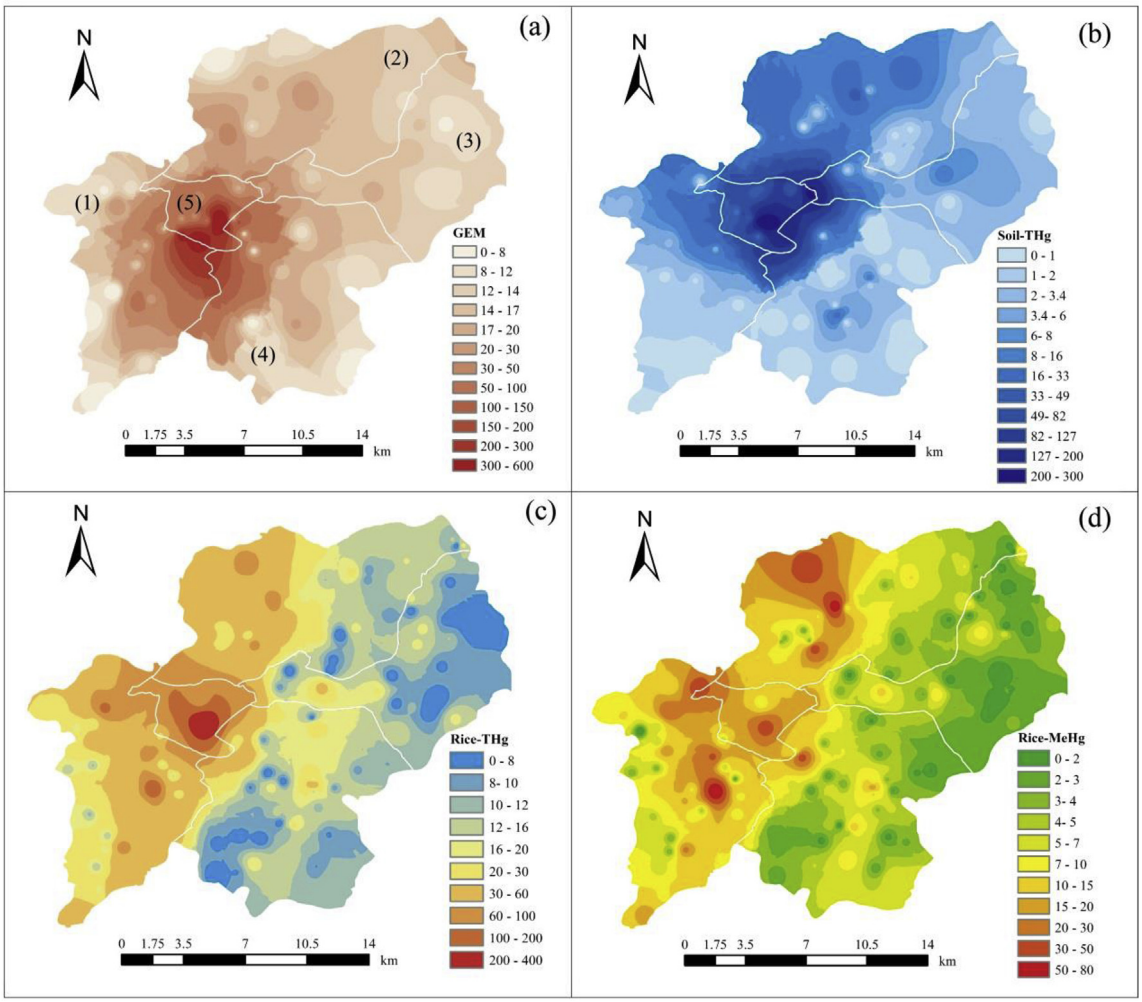

Fig. 1. The spatial distributions of Hg concentrations in soil, air, and rice in the WSMM. (a), (b), (c), and (d) show the spatial distributions of GEM in ambient air, THg in soil, THg, and MeHg in rice, respectively. The four villages and one town marked in (a) are (1) GLP, (2) AZ, (3) XX, (4) HD, and (5) WST.

consumption in the two zones were in different ranges of 2.16–164 ng kg^{-1} d^{-1} and 0.726–37.1 ng kg^{-1} d^{-1}. Among the average IHg PDIs of foodstuffs and drinking water, the vegetables consumption exhibited the highest PDI value (42.6 ng kg^{-1} d^{-1}), followed by consumption of pork (19.9 ng kg^{-1} d^{-1}), rice (4.19 ng kg^{-1} d^{-1}, GM), poultry (1.81 ng kg^{-1} d^{-1}), fish (0.495 ng kg^{-1} d^{-1}), and corn (0.142 ng kg^{-1} d^{-1}). And drinking water showed the lowest IHg PDI (0.107 ng kg^{-1} d^{-1}) in dietary pathways. Meanwhile, for MeHg, PDIs for rice consumption in the two zones were in different variations of 11.4–200 ng kg^{-1} d^{-1} and 2.41–468 ng kg^{-1} d^{-1}. As for the mean MeHg PDIs of dietary pathways, rice consumption showed the highest value (26.4 ng kg^{-1} d^{-1}, GM), followed by consumption of fish (1.74 ng kg^{-1} d^{-1}), pork (1.07 ng kg^{-1} d^{-1}), and poultry (0.275 ng kg^{-1} d^{-1}), while mean MeHg PDI of water drinking still was the lowest (0.002 ng kg^{-1} d^{-1}), suggesting a negligible exposure dose.

Soil. In this study, the Rba values in the normal and assumed scenarios were taken as 7% and 100%, respectively. The PDIs for oral ingestion of soil particles are listed in Table 2. We observed a significant decrease in PDI in the order of 0–4 km > 4–15 km for both children and adults in both scenarios. In the two zones and normal scenario, the PDIs of children were 0.636–283 (30.3, GM) ng kg^{-1} d^{-1} and 0.0422–35.7 (0.83, GM) ng kg^{-1} d^{-1}, while the PDIs of adults in the two zones were 0.0870–38.7 (4.14, GM) ng kg^{-1} d^{-1} and 5.77 × 10^{-3}–4.88 (0.113, GM) ng kg^{-1} d^{-1}, respectively. In comparison, the PDIs of both children and adults under the assumed scenario were much higher and even exceeded the RfD (300 ng kg^{-1} d^{-1}) and PTWI (570 ng kg^{-1} d^{-1}) of IHg. Meanwhile, for children with a soil-pica habit (IR 1000 mg d^{-1}) under the normal scenario, the PDI in the 0–4 km zone was elevated and even exceeded both the RfD and PTWI. Thus, oral ingestion of soil could pose significant exposure risks to local people, especially children with a soil-pica habit.

3.2.2. Inhalation

The PDI for GEM inhalation over the entire area was 0.242–153 (3.13, GM) ng kg^{-1} d^{-1}, which is comparable to that for the consumption of other foodstuffs. However, the PDI of PHg was 2.64 × 10^{-7}–1.77 × 10^{-3} (1.19 × 10^{-5}, GM) ng kg^{-1} d^{-1}, which is significantly lower than that for the inhalation of GEM, other oral ingestion pathways, and the reference dose of inhalation (RfD_{inh}, 72 ng kg^{-1} d^{-1} for adults) converted from the reference concentration and daily inhalation volume (MEE, 2014), suggesting that there is a negligible health risk to the local inhabitants.

3.2.3. Dermal contact

For soil particles, the PDIs in two zones were 4.27 × 10^{-3}–1.90 (0.203, GM) ng kg^{-1} d^{-1} and 2.84 × 10^{-4}–0.240 (5.53 × 10^{-3}, GM) ng kg^{-1} d^{-1}, respectively. The mean PDI of dermal contact with water was 1.71 × 10^{-3} ng kg^{-1} d^{-1}. The PDIs of both dermal contact pathways were much lower than the reference dose of dermal contact (RfD_{der}, 21 ng kg^{-1} d^{-1}) recommended by the USEPA (2019b), also suggesting negligible exposure risk.

3.3. Contribution rates of different exposure pathways

The probability distributions of the CRs were simulated by Monte Carlo simulation (100,000 iterations), and the normalized median values were used to represent the mean CRs (Table 3). For MeHg, the CRs of rice consumption were 92.7%, 86.3%, and 87.5% in two zones and the entire area, respectively. These proportions were followed by those for the consumption of vegetables (two zones 0.85% and 1.6%, entire area 1.4%), fish (two zones 3.4% and 6.4%, whole area 5.9%) and pork (two zones 2.1% and 3.9%, entire area 3.6%). Compared with previous exposure risk assessments for MeHg (Zhang et al., 2010), the CRs of rice consumption were slightly lower but the CRs of vegetables, fish, and pork consumption were slightly higher, which is probably due to the different IR values of rice and other foodstuffs with elevated Hg concentrations that were only collected in Hg mining-affected areas.

For IHg and entire area, the CRs of vegetables, pork, rice, and poultry consumption were 59.1%, 27.6%, 5.3%, and 2.5%, respectively. The total proportion of 94.5% suggests that the consumption of these four foodstuffs is the main IHg exposure pathway. The CR of GEM inhalation was 4.2% but the PHg inhalation and dermal contact CRs (both soil and water) were negligible (<0.02%). Compared with previous exposure risk assessments of IHg (Li et al., 2015a) and

Table 2
PDIs of IHg and MeHg of each exposure pathway in Wanshan (ng kg^{-1} d^{-1}).

Pathways		IHg (MeHg)[a]					
		0–4 km		4–15 km		Whole area	
		Range	GM/AM/P50/P95	Range	GM/AM/P50/P95	Range	GM/AM/P50/P95
Oral	Soil-a-n	0.0870–38.7	4.14/9.22/4.65/33.5	0.00577–4.88	0.113/0.392/0.114/2.36	0.0057–38.7	0.260/2.45/0.156/11.3
	Soil-*c*-n	0.636–283	30.3/67.4/34.0/283	0.0422–35.7	0.822/2.87/0.837/17.3	0.0422–283	1.90/17.9/1.14/82.5
	Soil-a-as	1.19–530	56.7/126/63.6/458	0.0791–66.9	1.54/5.49/1.57/32.3	0.0791–530	3.64/34.3/2.21/155
	Soil-*c*-as	9.08–4042	433/963/485/3493	0.603–510	11.8/41.9/12.0/246	0.603–4042	27.8/261/August 16, 1179
	Soil-*c*-sp	3.18–1415	151/337/170/1223	0.211–178	4.12/14.7/4.18/86.1	0.211–1415	9.71/91.4/5.88/413
	Rice	2.16–164 (**11.4–200**)	8.78/19.7/6.62/164 (**51.3/73.9/41.7/200**)	0.726–37.1 (**2.41–468**)	3.86/5.43/3.79/14.2 (**24.4/40.4/24.1/116**)	0.726–164 (**2.41–468**)	4.19/6.87/4.12/17.6 (**26.4/43.8/25.9/174**)
	Vegetables						42.6/(**4.32**)[b]
	Corn						0.142/(**0.235**)[b]
	Pork						19.9/(**1.07**)[b]
	Poultry						1.81/(**0.275**)[b]
	Fish						0.495/(**1.74**)[b]
	Water						0.107/(**0.002**)[b]
Inhalation	GEM	1.29–153	6.50/20.2/3.67/90.7	0.242–14.3	2.26/2.85/2.53/4.94	0.242–153	3.13/8.19/2.89/31.0
	PHg	3.97 × 10^{-6}-1.77 × 10^{-3}	1.89 × 10^{-4}/4.21 × 10^{-4}/2.12 × 10^{-4}/1.53 × 10^{-3}	2.64 × 10^{-7}-2.23 × 10^{-4}	5.14 × 10^{-6}/1.79 × 10^{-5}/5.23 × 10^{-6}/1.08 × 10^{-4}	2.64 × 10^{-7}-1.77 × 10^{-3}	1.19 × 10^{-5}/1.12 × 10^{-4}/7.13 × 10^{-6}/5.16 × 10^{-4}
Dermal	Soil	4.27 × 10^{-3}-1.90	0.203/0.453/0.228/1.64	2.84 × 10^{-4}-0.240	5.53 × 10^{-3}/0.0193/5.62 × 10^{-3}/0.116	2.84 × 10^{-4}-1.90	1.28 × 10^{-2}/0.120/7.66 × 10^{-3}/0.554
	Water						1.71 × 10^{-3}

[a] Bold data in brackets is MeHg.
[b] Mean value.

Table 3
CRs of exposure pathways of Hg in Wanshan.

Areas	Inhalation		Dermal contact		Oral ingestion								Sources
	GEM	PHg	Soil	Water	Soil	Water	Rice	Vegetables	Corn	Pork	Poultry	Fish	
THg or IHg													
Whole	1.3–4.7	–	–	–	–	0.1–0.2	18.6–23.7	46.1–53.7	0.2–0.3	16.9–25.9	1.1–1.7	0.3–0.5	Li et al. (2015a)
Whole[a]	1.64	–	–	–	–	0.09	42.2	40.5	0.09	14.7	0.66	0.30	Zhang et al. (2010)
Whole[a]	10.0	–	–	–	–	–	57.2	24.8	–	6.9	–	1.1	Du et al. (2016)
Whole[b]							95					5	Du et al. (2018)
0–4 km	6.14	2×10^{-4}	0.25	0.002	5.3	0.13	9.4	51.7	0.17	24.1	2.2	0.60	This study
4–15 km	3.5	7×10^{-6}	0.007	0.002	0.14	0.15	5.1	59.8	0.20	27.9	2.5	0.69	This study
Whole	4.2	2×10^{-5}	0.02	0.002	0.31	0.15	5.3	59.1	0.20	27.6	2.5	0.68	This study
MeHg													
Whole	–	–	–	–	–	0.002	96.6	0.62	0.26	1.2	0.2	1.26	Zhang et al. (2010)
0–4 km	–	–	–	–	–	0.004	92.7	0.85	0.46	2.1	0.54	3.4	This study
4–15 km	–	–	–	–	–	0.007	86.3	1.6	0.86	3.9	1.0	6.4	This study
Whole	–	–	–	–	–	0.006	87.5	1.4	0.79	3.6	0.92	5.9	This study

[a] Using THg.
[b] Using Hg isotope method, and 95% is non-fish foodstuffs, 5% is fish foodstuffs.

THg (Zhang et al., 2010; Du et al., 2016), our results showed lower CRs of rice consumption and GEM inhalation but higher CRs of vegetables, pork, poultry, and fish consumption. Aside from the possible causes of the MeHg CRs, the much higher CRs reported by Zhang et al. (2010) and Du et al. (2016) resulted from calculation of THg concentrations without consideration of absorption factors.

Notably, for oral ingestion of soil particles, a large variation (0.14–5.3%) in the IHg CRs in the two zones was observed, suggesting that this exposure pathway could generate a significantly higher IHg exposure risk in the heavily contaminated area. For the elevated CRs, we further analyzed the probability distributions of the CRs of soil particle oral ingestion with those of GEM inhalation and rice consumption in the two Hg contamination zones (0–4 km and 4–15 km) and the relationships between IHg (or THg) concentrations and PDIs in Fig. 2 (**c**) and (**d**). Both the probability distributions and the linear relationships reveal that the elevated CR (median = 4.65%) and exposure dose obtained from the oral ingestion of soil particles is comparable with those of GEM inhalation (median 6.14%) and rice consumption (median 9.43%) in the heavily Hg-contaminated area (0–4 km zone). Thus, the significant proportion of exposure due to oral ingestion of soil in the heavily contaminated area is reliable in Hg-mining areas.

3.4. Total exposure doses of IHg and MeHg

In the present study, the PDIs of IHg and MeHg were obtained by Monte Carlo simulation for the entire area and the two zones shown in Fig. 2 (a, b) and **S2**. If we assume that the probability distribution equals the entire exposure risk to local people, the IHg PDIs of about 0.2% and 0.06% residents exceed the RfD and PTWI values of the whole area, respectively. The two values in the 0–4 km zone are 2.37% and 0.58%, while nearly no people exceed the criteria in 4–15 km zone. Thus, the data indicate that only residents in the heavily Hg-contaminated area suffered elevated IHg exposure risks, while those of residents in the other areas were acceptable.

For MeHg, the PDIs of residents in the entire area of about 9.81% and 1.62% exceeded the two criteria of RfD and PTWI, respectively. For the two zones, the proportions were 23.8% and 6.6% (0–4 km zone, RfD and PTWI) and 7.74% and 1.2% (4–15 km zone, RfD and PTWI), respectively (Fig. S2). Thus, compared with IHg, elevated MeHg exposure risk was the most significant health issue for local people, especially the residents in heavily Hg-contaminated areas. Our results are also consistent with the investigation into MeHg concentrations in hair (8.2% and 2.1%) by Li et al. (2015b), but much lower than the 34% and 7% reported by Zhang et al. (2010).

4. Risk categorization and prioritization

For Hg-contaminated soil, the risk screening value (RCV) and risk control value (RSV) recommended by MEE (2018a, 2018b, 2019) for residential land are 33 mg kg^{-1} and 8 mg kg^{-1}, respectively, while the values for agricultural land are 6 mg kg^{-1} and 3.4 mg kg^{-1}. Thus, according to the soil Hg concentration, soil-areas 1, 2, 3, 4, and 5 can be divided according to the two criteria for residential and agricultural land (Fig. S3). The priority for treatment or remediation decreased from soil-areas 1 to 5, while and soil-area 1 and soil-areas 1–3 are the top priorities for residential and agricultural land, respectively.

Using the PDIs and CRs of rice consumption, the spatial distributions of the total PDIs of IHg and MeHg were obtained (Fig. 3). Similarly, based on the RfD and PTWI, three areas were categorized to represent higher (rice-areas 1 and 2) and lower (rice-area 3) exposure risk levels for both IHg and MeHg. The priority for treatment or remediation decreased from rice-areas 1 to 3. For both IHg and MeHg, rice-areas 1 and 2 were concentrated in areas near Hg mining and retorting sites (mainly in WST, AZ and GLP), but a difference was also observed in the distributions of elevated IHg and MeHg exposure dose areas. Unlike the IHg, rice-areas 1 and 2 of MeHg covered a larger area, mainly in the vicinity of Hg mines, chemical facilities, and previous retorting sites of WST, GLP and AZ. As newly deposited Hg is highly bioavailable to methylation in rice paddies (Zhao et al., 2016; Ao et al., 2020), the dissimilar distributions of IHg and MeHg might be related to strong methylation processes occurring in Hg mining or retorting impacted rice paddy ecosystems.

5. Suggested actions

Suggested actions for mitigating Hg-contaminated soil and elevated Hg exposure risks are listed in Table S2. For contaminated soil used for residential purposes, soil remediation or treatment should be conducted in soil-area 1, while a detailed investigation and risk assessment should be conducted in soil-area 2. For contaminated soil used for agricultural purposes, strict control measures (such as agronomic regulation and delimitation farming) should be undertaken in soil-areas 1, 2 and 3, while continuous monitoring and risk assessment should be conducted in soil-area 4. In addition, because oral ingestion of soil particles is an important IHg exposure pathway in heavily Hg-contaminated areas,

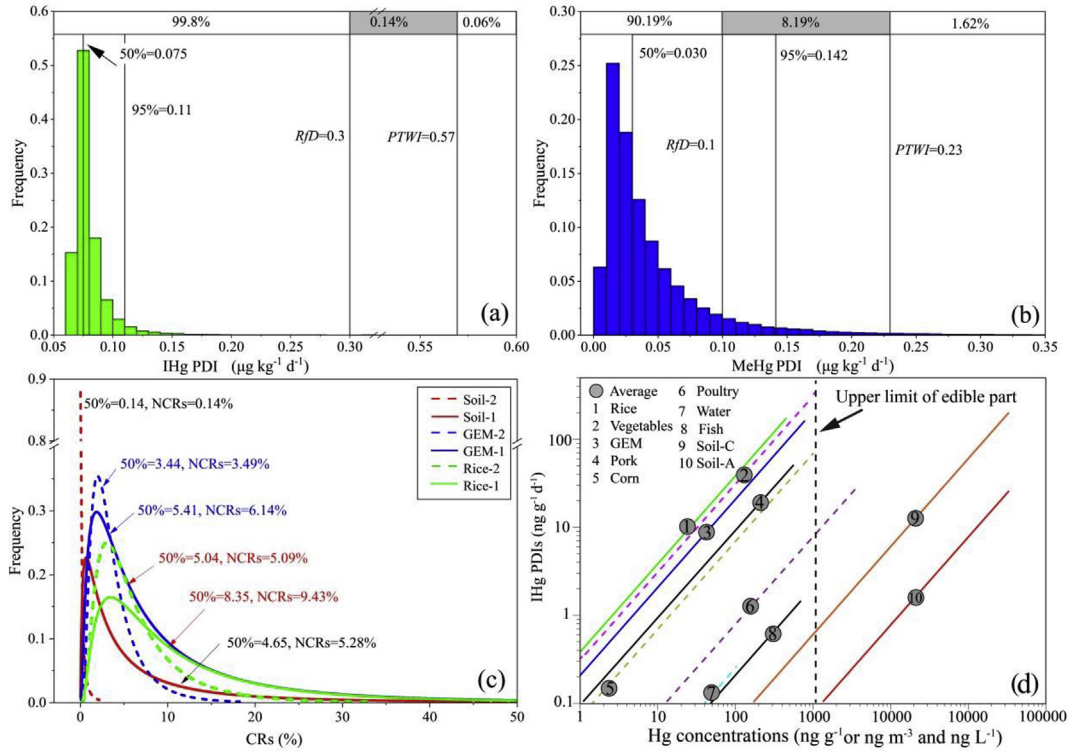

Fig. 2. Rice-based total exposure doses of (a) IHg and (b) MeHg; (c) frequency IHg CRs of oral soil ingestion, GEM inhalation, and rice consumption; and (d) Hg concentration versus IHg PDIs in the WSMM. For (c), 1 indicates the 0–4 km zone, 2 is the 4–15 km zone. For agricultural products in (d), THg was used to represent the upper limit of IHg concentrations, 1075 ng g^{-1} is the maximum THg in the edible parts of agricultural products recently reported by Xia et al. (2020). And 3917.1 ng g^{-1} is the maximum of THg in poultry recently reported by Yin et al. (2017). For drinking water, the national criteria of 100 ng L^{-1} in surface drinking water reported by MEE (2002) was used as the maximum THg concentration.

additional cleaning procedures, such as frequent hand washing and showering, are strongly recommended during outdoor activities around abandoned Hg mines and chemical plants, especially for children and toddlers who have a high frequency of hand-to-mouth activity.

In relation to elevated Hg exposure risks, since food consumption accounted for the highest proportions of IHg and MeHg exposure (95.4% and ~100%, respectively), one of most effective treatments would be to directly reduce local food consumption. As shown in Fig. 3, there is no imperative need to reduce the consumption of local foods in the eastern and southern parts of the WSMM (mainly in XX and HD), which had relatively low PDIs for both IHg and MeHg. However, for the western and northern areas (mainly in WST, AZ and GLP), which had higher PDIs for both IHg and MeHg, the consumption of local high-Hg foodstuffs, particularly rice, vegetables, and pork, should be strictly limited. Alternatively, commercial foods or other local foods with low Hg concentrations, like those cultivated in areas like XX and HD,

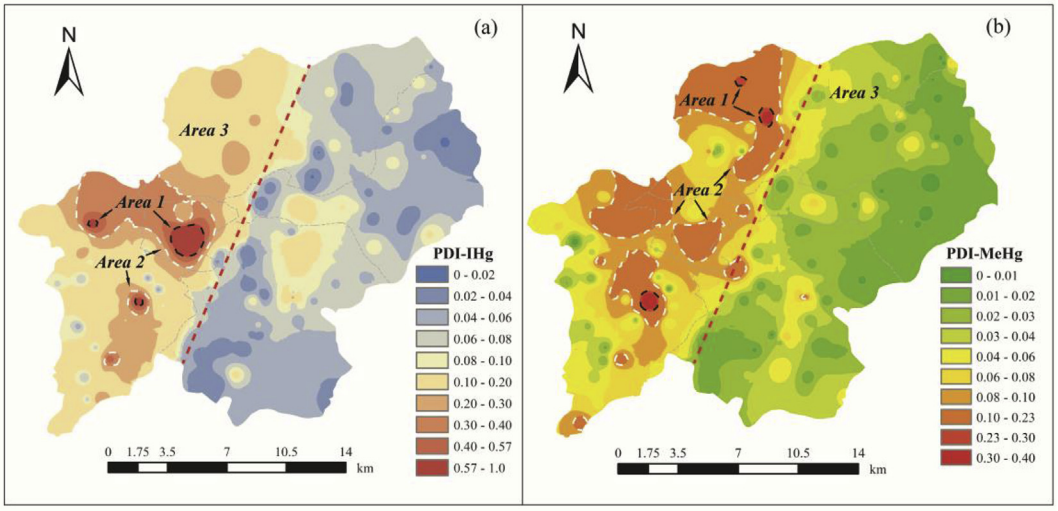

Fig. 3. Risk categorization and prioritization based on exposure doses of (a) IHg and (b) MeHg (areas representing high and low exposure risk are divided by red dotted lines).

should be consumed. This countermeasure of limiting the consumption of local foodstuffs with elevated Hg concentrations would be feasible and beneficial to local society.

6. Implications for the Minamata Convention

Article 12 of the Minamata Convention requires that HHRA and risk categorization and prioritization should be conducted at Hg-contaminated sites. Although technical guidelines for the risk assessment of contaminated sites, and RSVs and RCVs for contaminated soil in agricultural and developed land (residential and industrial) have been published by MEE (2014, 2018a, 2018b, 2019), current models and methods are mainly designed for industrially contaminated sites and rarely consider the food consumption exposure risk. In addition, values of certain exposure factors are not suitable for contaminated agricultural areas and need to be optimized. For example, the gastrointestinal tract absorption factor for soil Hg is usually regarded as 100%, rather than about 7%, which would overestimate exposure risk levels. Thus, current inconsistencies in knowledge of the absorption factors involved in different exposure pathways will cause large variations in estimates of exposure risk.

In the present study, the multi-pathway exposure model and its optimized exposure factor values were demonstrated to be suitable use in large-scale Hg-contaminated agricultural areas and presented reasonable Hg exposure risk estimates. In addition, with the help of Monte Carlo simulation and spatial distribution data on Hg-exposure risks, target areas and potential remediation or treatment actions were identified and prioritized. Thus, this pilot study on multi-pathway exposure could provide appropriate Hg exposure risk estimates that can inform future remediation or treatment programs at Hg mining contaminated areas. In addition, with the implementation of multi-pathways HHRA studies in other Hg-contaminated sites in future, the gaps existing in the current technical guidelines aspect would be narrowed significantly.

7. Conclusions

This study conducted a systematic pilot study of multi-pathway HHRA and risk categorization in Hg mining areas. Food consumption was the major exposure pathway for both MeHg and IHg. Elevated MeHg exposure risk was most significant issue in Hg mining areas, while IHg exposure risks were much lower than previously reported. Notably, unintentional oral ingestion of soil particles was also an important IHg exposure pathway in heavily Hg-contaminated areas that should not be ignored. Based on the spatial distributions of soil Hg concentrations and rice-based exposure doses of MeHg and IHg, various target areas of Hg-contaminated soil and Hg-exposure risk levels were also characterized and prioritized. Overall, the multi-pathway exposure model is suitable for Hg mining areas and is also strongly recommended for other types of Hg-contaminated sites worldwide (i.e. in the vicinity of chemical facilities and gold mining areas). This pilot study also is conducive to the current implementation of the Minimata Convention.

Declaration of competing interest

The authors declare that they have no known or potential competing financial interests.

Acknowledgements

This work was supported by the National Natural Science Foundation of China [NSFC, 41573135], the Sino-Norwegian Cooperative Project on Mercury Phase III [SINOMER III], the National Key Basic Research Program of China [2013CB430004] and China Post-doctoral Science Foundation [2019M663571]. We greatly thank the valuable comments from three anonymous reviewers, and also thank Ms. Min Yan, Ms. Le Wang and Dr. Axiang Cao for the great help in sampling and measurement in this study.

Appendix A. Supplementary data

Supplementary data to this article can be found online at https://doi.org/10.1016/j.chemosphere.2020.127582.

Author statements

Dr. Zhidong Xu: Investigation, Methodology, Writing-Original Draft, Visualization, Data process, Writing- Reviewing and Editing, Dr. Qinhui Lu: Investigation, Methodology, Monte Carlo Model operations, Dr. Xiaohang Xu: Investigation, Methodology, Funding acquisition. Prof. Xinbin Feng: Supervision, Dr. Longchao Liang: Investigation. Dr. Lin Liu: Investigation. Ms. Chan Li: Investigation. Prof. Zhuo Chen: Supervision Prof. Guangle Qiu: Supervision, Project administration, Funding acquisition. Ms. Min Yan, Ms. Le Wang, and Dr. Axiang Cao provided great help in sampling and measurement.

References

Ao, M., Xu, X.H., Wu, Y.G., Zhang, C., Meng, B., Shang, L.H., Liang, L.C., Qiu, R.L., Wang, S.H., Qian, X.L., Zhao, L., Qiu, G.L., 2020. Newly deposited atmospheric mercury in a simulated rice ecosystem in an active mercury mining region: high loading, accumulation, and availability. Chemosphere 238, 124630. https://doi.org/10.1016/j.chemosphere.2019.124630.

Árvay, J., Demková, L., Hauptvogl, M., Miloslav, M., Bajčan, D., Stanovič, R., Tomáš, J., Hrstková, M., Trebichalský, P., 2017. Assessment of environmental and health risks in former polymetallic ore mining and smelting area, Slovakia: spatial distribution and accumulation of mercury in four different ecosystems. Ecotoxicol. Environ. Saf. 144, 236–244. https://doi.org/10.1016/j.ecoenv.2017.06.020.

Bavec, Š., Biester, H., Gosar, M., 2018. A risk assessment of human exposure to mercury-contaminated soil and household dust in the town of Idrija (Slovenia). J. Geochem. Explor. 187, 131–140. https://doi.org/10.1016/j.gexplo.2017.05.005.

Chen, G.Z., Wang, X.M., Wang, R.W., Liu, G.J., 2019. Health risk assessment of potentially harmful elements in subsidence water bodies using a Monte Carlo approach: an example from the Huainan coal mining area. China. *Ecotoxicol. Environ. Saf.* 171, 737–745. https://doi.org/10.1016/j.ecoenv.2018.12.101.

China mineral processing technology mining website, 2017. The mercury ore reserves in China [In Chinese]. https://www.mining120.com/tech/show-htm-itemid- 27971.html. (Accessed 16 March 2020).

Deng, C.Y., Xie, H., Ye, X.J., Zhang, H.R., Liu, M.D., Tong, Y.D., Qu, L.B., Yuan, W., Zhang, W., Wang, X.J., 2016. Mercury risk assessment combining internal and external exposure methods for a population living near a municipal solid waste incinerator. Environ. Pollut. 219, 1060–1068. https://doi.org/10.1016/j.envpol.2016.09.006.

Dong, W.W., Zhang, Y., Quan, X., 2020. Health risk assessment of heavy metals and pesticides: a case study in the main drinking water source in Dalian, China. Chemosphere 242, 125113. https://doi.org/10.1016/j.chemosphere.2019.125113.

Du, B.Y., Li, P., Feng, X.B., Qiu, G.L., Zhou, J., Maurice, L., 2016. Mercury exposure in children of the wanshan mercury mining area, Guizhou, China. Int. J. Environ. Res. Publ. Health 13, 1107. https://doi.org/10.3390/ijerph13111107.

Du, B.Y., Feng, X.B., Li, P., Yin, R.S., Yu, B., Sonke, J.E., Guinot, B., Anderson, C.W.N., Maurice, L., 2018. Use of mercury isotopes to quantify mercury exposure sources in inland populations, China. Environ. Sci. Technol. 52, 5407–5416. https://doi.org/10.1021/acs.est.7b05638.

Eckley, C.S., Gilmour, C.C., Janssen, S., Luxton, T.P., Randall, P.M., Whalin, L., Austin, C., 2020. The assessment and remediation of mercury contaminated sites: a review of current approaches. Sci. Total Environ. 707, 136031. https://doi.org/10.1016/j.scitotenv.2019.136031.

Feng, X.B., Li, P., Qiu, G.L., Wang, S.F., Li, G.H., Shang, L.H., Meng, B., Jiang, H.M., Bai, W.Y., Li, Z.G., Fu, X.W., 2008. Human exposure to methylmercury through rice intake in mercury mining areas, Guizhou Province, China. Environ. Sci. Technol. 42, 326–332. https://doi.org/10.1021/es071948x.

Gibičar, D., Horvat, M., Logar, M., Fajon, V., Falnoga, I., Ferrara, R., Lanzillotta, E., Ceccarini, C., Mazzolai, B., Denby, B., Pacyna, J., 2009. Human exposure to mercury in the vicinity of chlor-alkali plant. Environ. Res. 109, 355–367. https://doi.org/10.1016/j.envres.2009.01.008.

GnamuŠ, A., Byrne, A.R., Horvat, M., 2000. Mercury in the soil-plant-deer-predator

food chain of a temperate forest in Slovenia. Environ. Sci. Technol. 34, 3337–3345. https://doi.org/10.1021/es991419w.
Gochfeld, M., 2003. Cases of mercury exposure, bioavailability, and absorption. Ecotoxicol. Environ. Saf. 56, 174–179. https://doi.org/10.1016/S0147-6513(03)00060-5.
Guney, M., Welfringer, B., Repentigny, C., Zagury, G.J., 2013. Children's exposure to mercury-contaminated soils: exposure assessment and risk characterization. Arch. Environ. Contam. Toxicol. 65, 345–355. https://doi.org/10.1007/s00244-013-9891-7.
Gyamfi, O., Sorenson, P.B., Darko, G., Ansah, E., Bak, J.L., 2020. Human health risk assessment of exposure to indoor mercury vapour in a Ghanaian artisanal small-scale gold mining community. Chemosphere 241, 125014. https://doi.org/10.1016/j.chemosphere.2019.125014.
JECFA (Joint Expert Committee on food), 2010. The Joint FAO/WHO Expert Committee on Food Additives Seventy- Second Meeting: Summary and Conclusions, pp. 1–16.
Ji, X.L., Hu, W.X., Cheng, J.P., Yuan, T., Xu, F., Qu, L.Y., Wang, W.H., 2006. Oxidative stress on domestic ducks (*Shaoxing duck*) chronically exposed in a Mercury–Selenium coexisting mining area in China. Ecotoxicol. Environ. Saf. 64, 171–177. https://doi.org/10.1016/j.ecoenv.2005.03.009.
Jia, Q., Zhu, X.M., Hao, Y.Q., Yang, Z.L., Wang, Q., Fu, H.H., Yu, H.J., 2018. Mercury in soil, vegetable and human hair in a typical mining area in China: implication for human exposure. J. Environ. Sci. 68, 73–82. https://doi.org/10.1016/j.jes.2017.05.018.
Jiménez-Oyola, S., Garía-Martínez, M., Ortega, M.F., Bolonio, D., Rodríguez, C., Esbrí, J., Llamas, J.F., Higuera, P., 2020. Multi-pathway human exposure risk assessment using Bayesian modeling at the historically largest mercury mining district. Ecotoxicol. Environ. Saf. 201, 110833. https://doi.org/10.1016/j.ecoenv.2020.110833.
Khpalwak, W., Jadoon, W.A., Abdel-dayem, S.M., Sakugawa, H., 2019. Polycyclic aromatic hydrocarbons in urban road dust, Afghanistan: implications for human health. Chemosphere 218, 517–526. https://doi.org/10.1016/j.chemosphere.2018.11.087.
Kocman, D., Horvat, M., Pirrone, N., Cinnirella, S., 2013. Contribution of contaminated sites to the global mercury budget. Environ. Res. 125, 160–170. https://doi.org/10.1016/j.envres.2012.12.011.
Li, P., Du, B.Y., Chan, H.M., Feng, X.B., 2015a. Human inorganic mercury exposure, renal effects and possible pathways in Wanshan mercury mining area, China. Environ. Res. 140, 198–204. https://doi.org/10.1016/j.envres.2015.03.033.
Li, P., Feng, X.B., Chan, H.M., Zhang, X.F., Du, B.Y., 2015b. Human body burden and dietary methylmercury intake: the relationship in a rice-consuming population. Environ. Sci. Technol. 49, 9682–9689. https://doi.org/10.1021/acs.est.5b00195.
Li, X.Y., Li, Z.G., Lin, C.J., Bi, X.Y., Liu, J.L., Feng, X.B., Zhang, H., Chen, J., Wu, T.T., 2018. Health risks of heavy metal exposure through vegetable consumption near a large-scale Pb/Zn smelter in central China. Ecotoxicol. Environ. Saf. 161, 99–110. https://doi.org/10.1016/j.ecoenv.2018.05.080.
Li, Y.H., 2013. Environmental contamination and risk assessment of mercury from a historic mercury mine located in southwestern China. Environ. Geochem. Health 35, 27–36. https://doi.org/10.1007/s10653-016-9864-7.
Li, F., Zhang, J.D., Jiang, W., Liu, C.Y., Zhang, Z.M., Zhang, C.D., Zeng, G.M., 2017. Spatial health risk assessment and hierarchical risk management for mercury in soils from a typical contaminated site, China. Environ. Geochem. Health 39, 923–934. https://doi.org/10.1007/s10653-016-9864-7.
Liang, L., Horvat, M., Cernichiari, E., Gelein, B., Balogh, S., 1996. Simple solvent extraction technique for elimination of matrix interferences in the determination of methylmercury in environmental and biological samples by ethylation-gas chromatography-cold vapor atomic fluorescence spectrometry. Talanta 43, 1883–1888. https://doi.org/10.1016/0039-9140(96)01964-9.
MEE Ministry of ecology and Environment of People's Republic of China, 2002. Environmental Quality Standards for Surface Water (GB 3838-2002).
MEE Ministry of ecology and Environment of People's Republic of China, 2012. Ambient Air Quality Standards (GB 3095-2012).
MEE Ministry of ecology and Environment of People's Republic of China, 2014. Technical Guidelines for Risk Assessment of Contaminated Sites (HJ 25.3-2014).
MEE Ministry of ecology and Environment of People's Republic of China, 2018a. Soil Environmental Quality Risk Control Standard for Soil Contamination of Agricultural Land (GB 15618-2018).
MEE Ministry of ecology and Environment of People's Republic of China, 2018b. Soil Environmental Quality Risk Control Standard for Soil Contamination of Development Land (GB 36600-2018).
Qiu, G.L., Feng, X.B., Wang, S.F., Shang, L.H., 2005. Mercury and methylmercury in riparian soil, sediments, mine-waste calcines, and moss from abandoned Hg mines in east Guizhou province, southwestern China. Appl. Geochem. 20, 627–638. https://doi.org/10.1016/j.apgeochem.2004.09.006.
MEE Ministry of ecology and Environment of People's Republic of China, 2019. Technical Guidelines for Risk Assessment of Soil Contamination of Land for Construction (HJ 25.3-2019).
NHC National health Commission of the People's Republic of China, 2017. Food Safety Standards, Limits of Contaminants in Food (GB 2762-12017).
Qiu, G.L., Feng, X.B., Wang, S.F., Fu, X.W., Shang, L.H., 2009. Mercury distribution and speciation in water and fish from abandoned hg mines in Wanshan, Guizhou province, China. Sci. Total Environ. 407, 5162–5168. https://doi.org/10.1016/j.scitotenv.2009.06.007.
Riaz, A., Khan, S., Muhammad, S., Liu, C.H., Shah, M.T., Tariq, M., 2017. Mercury contamination in selected foodstuffs and potential health risk assessment along the artisanal gold mining, Gilgit-Baltistan, Pakistan. Environ. Geochem. Health 40 (2), 625–635. https://doi.org/10.1007/s10653-017-0007-6.
Safruk, A.M., Berger, R.G., Jackson, B.J., Pinsent, C., Hair, A.T., Sigal, E.A., 2015. The bioaccessibility of soil-based mercury as determined by physiological based extraction tests and human biomonitoring in children. Sci. Total Environ. 518–519, 545–553. https://doi.org/10.1016/j.scitotenv.2015.02.089.
Shao, D.D., Wu, S.C., Liang, P., Kang, Y., Fu, W.J., Zhao, K.L., Cao, Z.H., Wong, M.H., 2012. A human health risk assessment of mercury species in soil and food around compact fluorescent lamp factories in Zhejiang Province, PR China. J. Hazard Mater. 221–222, 28–34. https://doi.org/10.1016/j.jhazmat.2012.03.061.
Sun, G.Y., Feng, X.B., Yang, C.M., Zhang, L.M., Yin, R.S., Li, Z.G., Bi, X.Y., Wu, Y.J., 2020. Levels, sources, isotope signatures, and health risks of mercury in street dust across China. J. Hazard Mater. 122276 https://doi.org/10.1016/j.jhazmat.2020.122276.
UNEP United Nations Environment Programme, 2017. Minamata Convention on Mercury-Text and Annexes. http://www.mercuryconvention.org/Portals/11/documents/Booklets/COP1%20version/Minamata-Convention-booklet-eng-full.pdf.
USEPA the United States Environmental Protection Agency, 2001. Method 1630: Methyl Mercury in Water by Distillation, Aqueous Ethylation, Purge and Trap, and CVAFS. Draft January 2001, vol. 4303. U.S. Environmental Protection Agency, Office of Water, Office of Science and Technology Engineering and Analysis Division, pp. 1–41, 20460.
USEPA the United States Environmental Protection Agency, 2002. Method 1631: Mercury in Water by Oxidation, Purge and Trap, and Cold Vapor Atomic Fluorescence Spectrometry. USEPA, Washington, DC, USA, pp. 1–33.
USEPA the United States Environmental Protection Agency, 2004. Risk assessment guidance for superfund (rags), volume i: human health evaluation manual (part e, supplemental guidance for dermal risk assessment) interim, pp. 1–156.
USEPA the United States Environmental Protection Agency, 2019a. EPA ExpoBox. https://www.epa.gov/expobox/exposure-assessment-tools-routes.
USEPA the United States Environmental Protection Agency, 2019b. Handbook of Exposure Factors. https://www.epa.gov/expobox/about-exposure-factors-handbook.
Wang, J.X., Feng, X.B., Anderson, C.W.N., Xing, Y., Shang, L.H., 2012. Remediation of mercury contaminated sites – a review. J. Hazard Mater. 221–222, 1–18. https://doi.org/10.1016/j.jhazmat.2012.04.035.
Wanshan Government, 2019. The Introduction of Wanshan District [In Chinese]. http://www.trws.gov.cn/zjws/. (Accessed 16 March 2020).
Xia, J.C., Wang, J.X., Zhang, L.M., Anderson, C.W.N., Wang, X., Zhang, H., Dai, Z.H., Feng, X.B., 2020. Screening of native low mercury accumulation crops in a mercury polluted mining region: agricultural planning to manage mercury risk in farming communities. J. Clean. Prod. 262, 121324. https://doi.org/10.1016/j.jclepro.2020.121324.
Xu, X.H., Han, J.L., Pang, J., Wang, X., Lin, Yan, Wang, Y.J., Qiu, G.L., 2020. Methylmercury and inorganic mercury in Chinese commercial rice: implications for overestimated human exposure and health risk. Environ. Pollut. 258, 113706. https://doi.org/10.1016/j.envpol.2019.113706.
Yin, R.S., Zhang, W., Sun, G.Y., Peng, Z.H., Hurley, J.P., Yang, L.Y., Shang, L.H., Feng, X.B., 2017. Mercury risk in poultry in the wanshan mercury mine, China. Environ. Pollut. 230, 810–816. https://doi.org/10.1016/j.envpol.2017.07.027.
Zhang, H., Feng, X.B., Larssen, T., Qiu, G.L., Vogt, R.D., 2010. In inland China, rice, rather than fish, is the major pathway for methylmercury exposure. Environ. Health Perspect. 1183–1188 https://doi.org/10.1289/ehp.1001915.
Zhao, L., Qiu, G.L., Anderson, C.W.N., Meng, B., Wang, D.Y., Shang, L.H., Yan, H.Y., Feng, X.B., 2016. Mercury methylation in rice paddies and its possible controlling factors in the Hg mining area, Guizhou province, Southwest China. Environ. Pollut. 215, 1–9. https://doi.org/10.1016/j.envpol.2016.05.001.